Journal of Hazardous Materials 164 (2009) 923–928

Contents lists available at ScienceDirect

Journal of Hazardous Materials

journal homepage: www.elsevier.com/locate/jhazmat

Adsorption behavior of multiwall carbon nanotube/iron oxide magnetic composites for Ni(II) and Sr(II)

Changlun Chen*, Jun Hu, Dadong Shao, Jiaxing Li, Xiangke Wang*

Institute of Plasma Physics, Chinese Academy of Sciences, P.O. Box 1126, Hefei 230031, Anhui, PR China

ARTICLE INFO

Article history:
Received 1 July 2008
Received in revised form 24 August 2008
Accepted 26 August 2008
Available online 2 September 2008

Keywords:
Multiwall carbon nanotube
Magnetic composites
Adsorption
Ni(II)
Sr(II)

ABSTRACT

Multiwall carbon nanotube (MWCNT)/iron oxide magnetic composites were prepared, and were characterized by scan electron microscopy using a field emission scanning electron microscope, X-ray diffraction and vibrating sample magnetometer. The adsorptions of Ni(II) and Sr(II) onto MWCNT/iron oxide magnetic composites were studied as a function of pH and ionic strength. The results show that the adsorptions of Ni(II) and Sr(II) on the magnetic composites is strongly dependent on pH and ionic strength. The adsorption capacity of the magnetic composites is much higher than that of MWCNTs and iron oxides. The solid magnetic composites can be separated from the solution by a magnetic process. The Langmuir model fits the adsorption isotherm data of Ni(II) better than the Freundlich model. Results of desorption study shows that Ni(II) adsorbed onto the magnetic composites can be easily desorbed at pH < 2.0. MWCNT/iron oxide magnetic composites may be a promising candidate for pre-concentration and solidification of heavy metal ions and radionuclides from large volumes of aqueous solution, as required for remediation purposes.

1. Introduction

Carbon nanotubes (CNTs) [1] have come under intense multidisciplinary study because of their unique physical and chemical properties. CNTs include single-wall (SWCNTs) and multiwall (MWCNTs) depending on the number of layers comprising them. They have been used to adsorbents for hydrogen and other gases due to their highly porous and hollow structure, large specific surface area, light mass density and strong interaction between carbon and hydrogen molecules [2–7]. CNTs have been found as efficient adsorbents for dioxin [8]. The adsorption capacity of CNTs was superior to that of activated carbon attributed to the stronger interactions between dioxins and CNTs. Liu et al. [9] reported that CNTs filled with gallium could be used as highly sensitive metal vapor sensors and absorbents, and copper vapor not only could deposit into open CNTs but also get into closed CNTs. Yang et al. [10] reported adsorption of polycyclic aromatic hydrocarbons by C_{60} fullerene, SWCNTs and MWCNTs. Yan et al. [11] reported adsorption of microcystins by CNTs. There are still a few reports on CNTs application for heavy metal ion and radionuclide treatment [12–20]. The earlier studies indicated that CNTs may be a promising adsorption material used in the waste treatment.

Because of their relatively large specific area, CNTs can be used as supports for catalyst and adsorption materials [21–26]. The application of magnetic particle technology to solve environmental problems has received considerable attention in recent years. Magnetic particles can be used to adsorb contaminants from aqueous or gaseous effluents and, after adsorption, can be separated from the medium by a simple magnetic process. Examples of this technology are the use of magnetite particles to accelerate the coagulation of sewage [27], a magnetite-coated functionalized polymer such as a resin to remove radionuclides from milk [28], the magnetic particles coated poly(oxy-2,6-dimethyl-1,4-phenylene) for the adsorption of organic dyes [29] and polymer-coated magnetic particles for oil spill remediation [30]: an experiment in environmental technology. However, all these materials have the drawback of a small surface area or a small adsorption capacity, which limits their application.

Removals of heavy metal ions and radionuclides from waste solutions are an important environmental concern in waste management. The objectives of this study are: (1) to prepare and characterize MWCNT/iron oxide magnetic composites, and (2) to investigate the adsorption behavior of Ni(II) and Sr(II) on the magnetic composites as a function of pH and ionic strength. Nickel is a toxic metal ion present in wastewater. More than 40% of nickel produced is used in steel factories, in nickel batteries and in the production of some alloys, which causes an increase in the Ni(II) burden on the ecosystem and deterioration water quality.

* Corresponding authors. Fax: +86 551 5591310.
E-mail addresses: clchen@ipp.ac.cn (C. Chen), xkwang@ipp.ac.cn (X. Wang).

0304-3894/$ – see front matter © 2008 Published by Elsevier B.V.
doi:10.1016/j.jhazmat.2008.08.089

Moreover, ^{63}Ni is a decay product of fission reactor facilities. Strontium is chosen as a divalent fission product, susceptible to being present in nuclear repositories.

2. Experiment

2.1. Preparation and characterization of MWCNT/iron oxide magnetic composites

MWCNTs were synthesized by using chemical vapor deposition (CVD) of acetylene in hydrogen flow at 760 °C using Ni–Fe nanoparticles as catalysts. ($Fe(NO_3)_2$ and $Ni(NO_3)_2$ were treated by sol–gel process and calcinations to get FeO and NiO, and then deoxidized doubly by H_2 to get Fe and Ni [17,18]. Oxidized MWCNTs were prepared by oxidization with 3 M HNO_3 [17,18]. Briefly, 400 mL 3 M HNO_3 including 2 g of MWCNTs was ultrasonically stirred for 24 h, filtrated, rinsed with doubly distilled water until the pH reached about 6, dried overnight in the oven at 80 °C, and then calcined at 450 °C for 4 h. Oxidized MWCNTs were well characterized in earlier reports [17,18].

The magnetic composites were prepared from a suspension of 1.0 g oxidized MWCNTs in a 150 mL solution of 2.98 g $FeCl_3{\cdot}6H_2O$ and 1.53 g $FeSO_4{\cdot}7H_2O$ at 70 °C under N_2 condition. NaOH solution (30 mL, 0.5 mol L^{-1}) was added dropwise to precipitate iron oxides. After the addition of NaOH solution, the mixture was adjusted to pH 11 and stirred for 1 h. The mixture was aged at 70 °C for 4 h and was washed 3 times with doubly distilled water. The obtained materials were dried in an oven at 100 °C for 3 h. The relevant chemical reactions can be expressed as follows:

$$Fe^{2+} + 2Fe^{3+} + 8OH^- + MWCNT \rightarrow MWCNT/Fe_3O_4 + 4H_2O \quad (1)$$

$$2Fe^{3} + 5OH^- + MWCNT \rightarrow MWCNT/Fe_2O_3 + 2H_2O + H^+ \quad (2)$$

Using the N_2-BET method, the specific surface area of MWCNT/iron oxide magnetic composites was 88.53 $m^2\,g^{-1}$. The magnetic composites were characterized by scan electron microscopy (SEM) using a field emission scanning electron microscope (FEI-Sirion 200), X-ray diffraction (XRD) and vibrating sample magnetometer (VSM). The morphological structures of the magnetic composites were performed using a JSM-840 scan electron microscope (Japan). Magnetic curves were obtained by Model-155 VSM at room temperature, and its measurement range is 0− ± 20.0 KOe. XRD measurements were performed by D/Max-2400 Rigaku X-ray powder diffractometer operated in the reflection mode with Cu Kα (λ = 0.15418 nm) radiation.

2.2. Batch adsorption experiment

The adsorptions of Ni(II) and Sr(II) on adsorbent were investigated by using batch technique in polyethylene centrifuge tubes sealed with screw-cap under N_2 condition at $T = 25 \pm 2$ °C in the presence of 0.01 and 0.1 M $NaClO_4$, respectively. The stock suspensions of adsorbent and $NaClO_4$ were pre-equilibrated for 24 h, and then Ni(II) or Sr(II) stock solution and radiotracer were added to achieve the desired concentration of the different components, and finally $HClO_4$ or NaOH was added to adjust pH values. The test tubes were shaken for 2 days to get the equilibrium state, and then 2 mL suspension was taken to get the total activity (A_{tot}), and the adsorbent in remaining suspension was separated by centrifugation of 18000 rpm for 30 min or by a magnetic process using a permanent magnet made of Nd–Fe–B for the analysis of the supernatant solutions (A_L). The pH of the supernatant was measured. The counting of ^{63}Ni(II) and ^{90}Sr(II) was analyzed by liquid scintillation counting using a Packard 3100 TR/AB Liquid scintillation analyzer (PerkinElmer) with the scintillation cocktail (ULTIMA GOLD AB™, Packard). The quenching effect arising from the presence of adsorbents on the counting was less than 4%, which is considered in the process of calculation. The adsorption percentage R was calculated according to $R(\%) = 100 \times (1 - A_L/A_{tot})$, herein, A_{tot} and A_L represent the activities of the suspension and those of the supernatant, respectively.

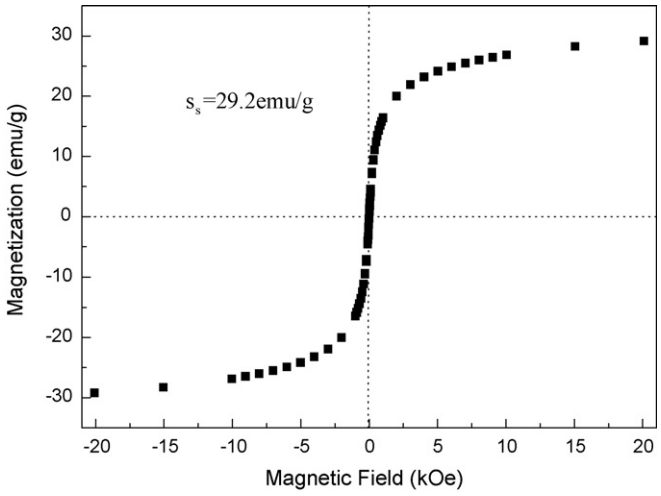

Fig. 1. Magnetization curve of the magnetic composites.

To investigate the desorption ability of adsorbed Ni(II) from MWCNT/iron oxide magnetic composites, desorption experiments were carried out as follows: after the adsorption reached equilibrium at initial pH 6.5 and ionic strength 0.01 M $NaClO_4$, the magnetic composites adsorbing Ni(II) ions were separated from the suspension and were slightly washed with doubly distilled water to remove un-adsorbed Ni(II) ions on the magnetic composites and then dried at 80 °C. The achieved magnetic composites with adsorbed Ni(II) were dispersed into 200 mL 0.01 M $NaClO_4$ and then each 20 mL suspension was removed to test tubes. The pH values of the solution were adjusted from about 6.2 to 1.6 using 0.1 M HNO_3. After 1 day's shaking, the Ni(II) released from the magnetic composites were measured as the measurement of Ni(II) in adsorption experiments, and the desorption data were then obtained from the concentration of free Ni(II) in the supernatant.

3. Results and discussion

3.1. Results of characterization of magnetic composites

After the preparation, a test with the Nd–Fe–B magnet showed that the whole material is magnetic and completely attracted to the magnet. The magnetization measurements show that the specific saturation magnetization σ_s is 29.2 emu g^{-1} (magnetic field = ±20 kOe) (Fig. 1). The X-ray diffraction patterns (Fig. 2) of the magnetic composites indicate that two peaks corresponding to the structure of MWCNTs also exist in the XRD pattern of the magnetite composites and the XRD pattern of the magnetic composites reveals a cubic iron oxide phase (2θ = 30.21, 35.49, 43.14, 53.33, 57.27, and 62.75, which are close to JCPD standards: Fe_3O_4, magnetite (89–3854, 2θ = 30.088, 35.439, 43.07, 53.432, 56.958, and 62.546), or γ-Fe_2O_3 (89–5892, 2θ = 30.266, 35.651, 43.332, 53.766, 57.319, and 62.949). Other peaks are observed at 2θ = 21.13, 33.26, 41.22, and 58.98) for the magnetic composites, which may be related to the presence of α-FeO(OH) (goethite) [31]. Fig. 3A and B shows the SEM images of oxidized MWCNTs and the magnetic composites, respectively. SEM image (Fig. 3B) of the composites depicts an entangled network of oxidized MWCNTs with clusters

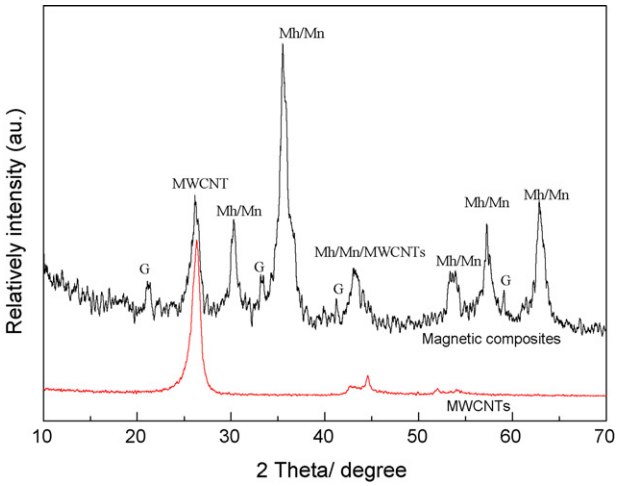

Fig. 2. XRD patterns of oxidized MWCNTs and the magnetic composites (Mh = maghemite, Mn = magnetite, and G = α-FeO(OH)).

of iron oxides attached to them, which indicates the formation of MWCNT/iron oxide magnetic composites.

3.2. Effect of shaking time

Fig. 4 shows the effect of the shaking time on Ni(II) adsorption onto MWCNT/iron oxide magnetic composites. The equilibrium is

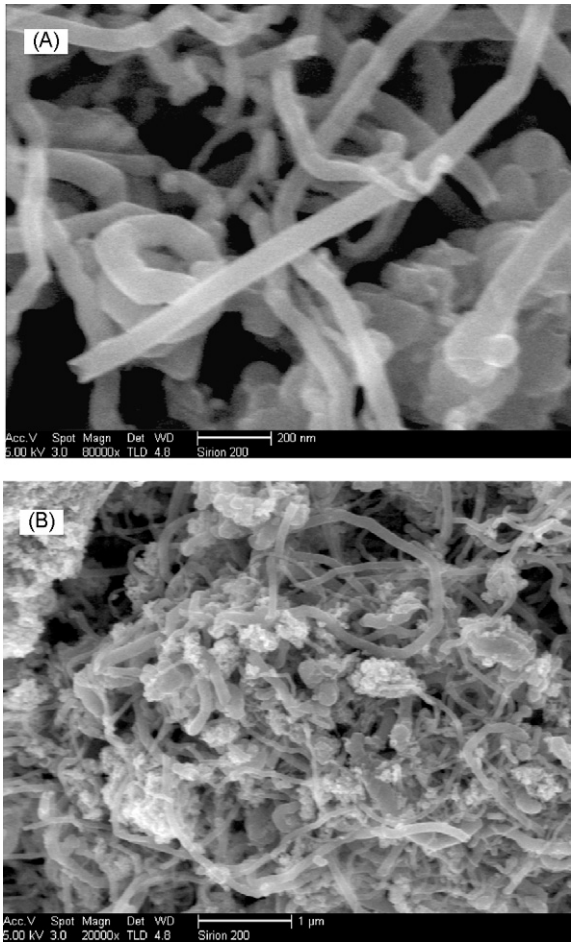

Fig. 3. SEM images of oxidized MWCNTs (A) and the magnetic composites (B).

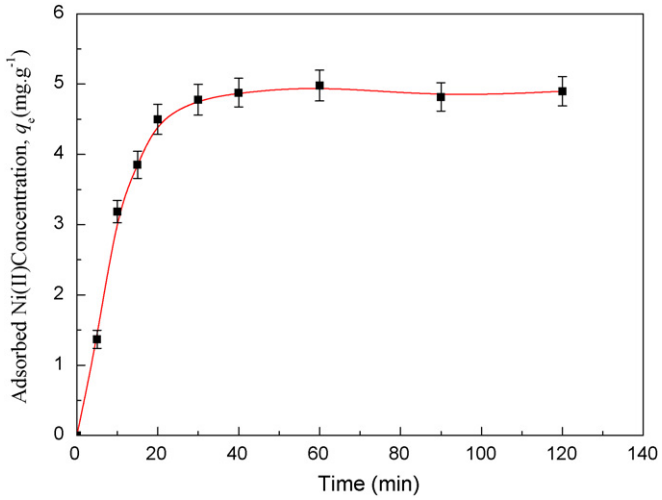

Fig. 4. Effect of shaking time on Ni(II) adsorption rate onto the magnetic composite, at $C_{initial}$[Ni(II)] = 6.0 mg L^{-1}, pH = 6.4 ± 0.2, I = 0.01 M $NaClO_4$, m/V = 0.75 g L^{-1}, and T = 25 ± 2 °C.

reached within 40 min in this study. It is necessary to note that the time in x-axis (Fig. 4) was the shaking time, and the centrifugation time (30 min) was not considered in the analysis of time dependent adsorption of Ni(II) on the magnetic composites. This result is very interesting because equilibrium time is one of the parameters for economical wastewater treatment plant applications. The implication is that the material could be suitable for a continuous flow system. According to the above results, the shaking time was fixed for 24 h for the rest of the batch experiments to assure that equilibrium was fully reached.

3.3. Effect of pH and ionic strength on adsorption

The solution pH is one of the dominant parameter controlling adsorption. Ni(II) and Sr(II) adsorptions onto MWCNT/iron oxide magnetic composites as a function of pH are given in Figs. 5 and 6. The adsorption of Ni(II) by the magnetic composites is highly dependent on pH. The adsorption of Ni(II) increases from ~10% (pH 3.5) to ~80% (pH 8.0). At higher pH values, metal ion hydroxides precipitation may account for metal ion removal. The K_{sp} value for

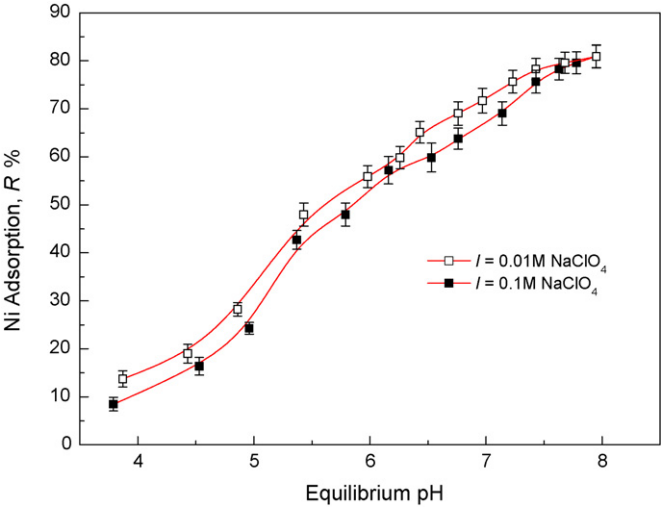

Fig. 5. Effect of ionic strength on Ni(II) adsorption onto the magnetic composites as a function of pH, at $C_{initial}$[Ni(II)] = 6.0 mg L^{-1}, m/V = 0.75 g L^{-1}, and T = 25 ± 2 °C.

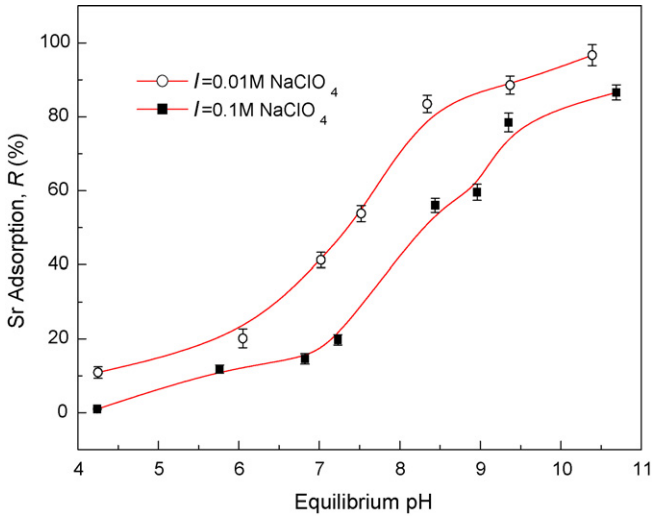

Fig. 6. Effect of ionic strength on Sr(II) adsorption onto the magnetic composites as a function of pH, at $C_{initial}$[Sr(II)] = 0.018 mg L^{-1}, m/V = 0.6 g L^{-1} and T = 25 ± 2 °C.

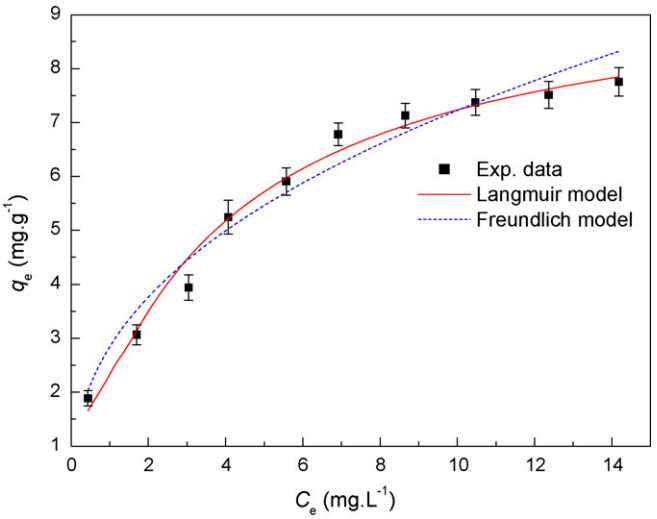

Fig. 7. Ni(II) adsorption isotherm onto the magnetic composites, at pH = 6.4 ± 0.2, I = 0.01 M $NaClO_4$, m/V = 0.75 g L^{-1}, and T = 25 ± 2 °C.

$Ni(OH)_2$ at 25 °C is 6.36×10^{-16}. The initial concentration used in this study is 6.0 mg L^{-1}, and therefore the pH where the hydroxides of Ni(II) begin to form is about 8.2. Within the pH range studied, no $Ni(OH)_2$ precipitation occurs and the removal of Ni(II) is due to adsorption.

According to Sr(II) hydrolysis constants: $\log \beta_1 = -13.29$ and $\log \beta_2 = -28.51$ [32], in 0.01 M $NaClO_4$ solution, only Sr^{2+} specie is present at a significant concentration in the pH range from 2 to 10, the $SrOH^+$ specie can be negligible between pH 2 and 10, and increases in concentration above 10 and becomes the predominant specie above pH 13. Fig. 6 shows Sr(II) adsorption onto the magnetic composites as a function of pH at two different ionic strengths. Sr(II) adsorption increases with increasing pH, and decreases with increasing ionic strength. Sr(II) was displayed a weak affinity for the magnetic composites at low pH, suggesting it does not easily form complexes with protonated magnetic composite functional groups. At pH values below the pH where metal ion hydroxide precipitation begins to formulate, the decreased adsorption with the decrease of pH may be due to positive surface charge caused by the protonation of electron π rich regions on the surface of the magnetic composites. A bond may be established with H_3O^+ ions and the cloud of π electrons of the aromatic rings of carbon and positive surface charge will be formed [33,34].

As pH increases, functional groups are progressively deprotonated, forming negative oxidized MWCNTs charge. The attractive forces between the anionic surface sites and cationic metal ions easily result in the formation of metal–ligand magnetic composite complexes.

The ionic strengths of 0.01 and 0.1 M $NaClO_4$ were chosen to investigate their effect on Ni(II) and Sr(II) adsorptions on MWCNT/iron oxide magnetic composites. Figs. 5 and 6 show that Ni(II) and Sr(II) adsorptions decrease with increasing ionic strength. This phenomenon could be attributed to two reasons: (1) Ni(II)/Sr(II) ions form electrical double layer complexes with the magnetic composites, which favored the adsorption when the concentration of the background electrolyte was decreased. This may imply that the adsorption interaction between the functional groups of the magnetic composites and metal ions was mainly ionic interaction nature, which was in good agreement with an ion exchange mechanism; (2) ionic strength of solution influenced the activity coefficient of metal ions, which limited their transfer to the composite surfaces [18,35].

After the adsorption, the magnetic separation process using the permanent magnet shows that the magnetic adsorbent can be easily separated from water and a recovery rate of above 97% has been achieved. Experiment tested that efficiency of magnetic separation was similar to that of centrifugation separation.

3.4. Adsorption isotherm model analysis

Fig. 7 shows the adsorption isotherm of Ni(II) on the magnetic composites. The experimental data of Ni(II) adsorption were analyzed with the Langmuir and Freundlich models [18]. The equations of the Langmuir and Freundlich adsorption models are expressed respectively by:

$$\frac{C_e}{q_e} = \frac{C_e}{Q_0} + \frac{1}{Q_0^b} \quad (1)$$

$$\ln q_e = \frac{\ln K + 1}{n \ln C_e} \quad (2)$$

where C_e (mg L^{-1}) is the concentration of Ni(II) in supernatant after adsorption and separation, q_e (mg g^{-1} of dry mass) is the equilibrium adsorption capacity, Q_0 (mg g^{-1}) is the adsorption maximum, b, K, and $1/n$ are isotherm constants. The value of K can be correlated to the adsorption capacity of an adsorbent under particular experimental conditions. The slopes and intercepts of the linear Langmuir and Freundlich plots are used to calculate the Langmuir and Freundlich constants tabulated in Table 1. From Table 1, higher correlation coefficients indicate that the Langmuir model fitted the adsorption data better than the Freundlich model.

3.5. Comparison with other adsorbents

Adsorption capacity of MWCNT/iron oxide magnetic composites for Sr(II) is compared with that of MWCNTs and iron oxides (Fig. 8). It can be seen that the adsorption capacity of the magnetic

Table 1
Parameters of the Langmuir and Freundlich models

Langmuir constants			Freundlich constants		
Q_0(mg g^{-1})	b(L mg^{-1})	R^2	K(mg$^{1-1/n}$ L$^{1/n}$ g^{-1})	$1/n$	R^2
9.18	0.37	0.986	2.85	0.404	0.962

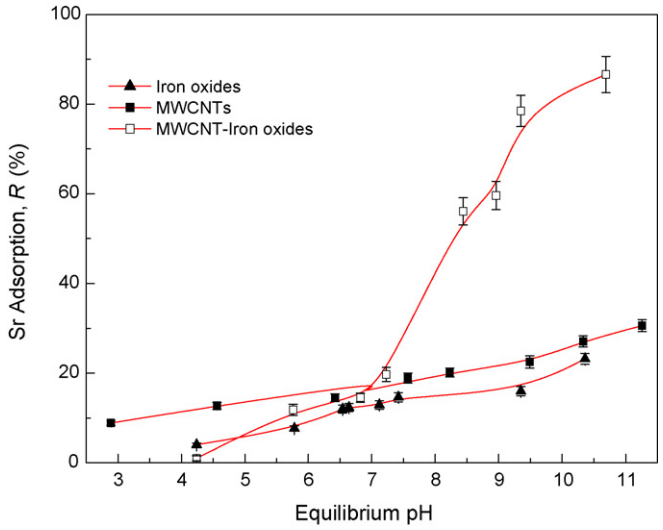

Fig. 8. Comparation of Sr(II) adsorption on MWCNTs, iron oxides and the magnetic composites, at $C_{initial}$[Sr(II)] = 0.018 mg L^{-1}, m/V = 0.6 g L^{-1}, I = 0.01 M $NaClO_4$, and T = 25 ± 2 °C.

composites for Sr(II) is higher than that of MWCNTs and iron oxides at pH > 7. The preparation process of iron oxides is the same as that of the magnetic composite. The specific surface area of iron oxides, 56.78 m^2 g^{-1}, is lower than that of the magnetic composites, 88.53 m^2 g^{-1}. Therefore, adsorption capacity of the magnetic composites for Sr(II) is higher than that of iron oxides at pH > 7. The reason why adsorption capacity of the magnetic composites for Sr(II) is higher than that of oxidized MWCNTs at pH > 7 is not however fully understood at the present time. Maybe, the synergistic effect between oxidized MWCNTs and iron oxides improves the adsorption capacity of the magnetic composites.

3.6. Desorption of Ni(II) from the magnetic composites

Repeated availability is an important factor for an advanced adsorbent. Such adsorbent not only possesses higher adsorption capability, but also shows better desorption property, which will significantly reduce the overall cost for the adsorbent. Fig. 9 shows the Ni(II) desorption percentages with regard to solutions at various pH values. It is apparent that Ni(II) desorption increases with decreasing of pH. About 12% of Ni(II) is desorbed from the magnetic composite at pH > 5.5, then increases sharply at pH < 5.0, and eventually reaches about 85% at pH < 2.0. Results show that the Ni(II) adsorbed by the magnetic composite could be easily desorbed, and thereby MWCNT/iron oxide magnetic composites can be employed repeatedly in wastewater management. Furthermore, this recovery also indicated that ion exchange was involved in the adsorption mechanism.

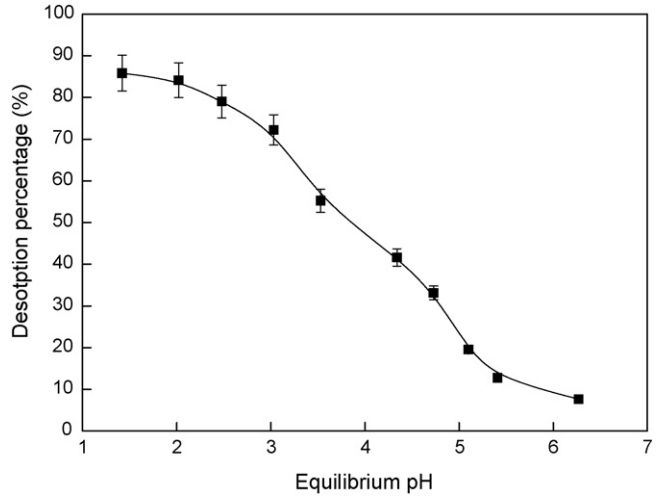

Fig. 9. Desorption of Ni(II) from the magnetic composites adjusting the pH of the solution using HNO_3 solution, at m/V = 0.75 g L^{-1}, and T = 25 ± 2 °C.

4. Conclusion

The magnetic composites can be prepared with a high adsorption capacity MWCNTs. XRD characterization suggests that the magnetic phase formed is maghemite or magnetite. SEM image shows an entangled network of MWCNTs with clusters of iron oxides attached to them and suggests the formation of MWCNT/iron oxide magnetic composites. Ni(II) adsorption on the magnetic composites is pH and ionic strength dependent. The Langmuir model fitted the adsorption isotherm data of Ni(II) better than the Freundlich model. The adsorption capacity of the magnetic composites for Sr(II) is higher than that of MWCNTs and iron oxides at pH > 7. Ni(II) can be easily desorbed from the magnetic composites by adjusting the solution pH values.

Acknowledgements

Financial support from the Natural Science Foundation of China (20677058) and Ministry of Science and Technology of China (2007CB936602) is acknowledged.

References

[1] S. Iijima, Helical microtubules of graphic carbon, Nature (Lond.) 354 (1991) 56–58.
[2] C. Kim, Y.S. Choi, S.M. Lee, J.T. Park, B. Kim, Y.H. Lee, The effect of gas adsorption on the field emission mechanism of carbon nanotubes, J. Am. Chem. Soc. 124 (2002) 9906–9911.
[3] R. Ma, Y. Bando, H. Zhu, T. Sato, C. Xu, D. Wu, Hydrogen uptake in boron nitride nanotubes at room temperature, J. Am. Chem. Soc. 124 (2002) 7672–7673.
[4] C. Liu, Y.Y. Fan, M. Liu, H.T. Cong, H.M. Cheng, M.S. Dresselhaus, Hydrogen storage in single-walled carbon nanotubes at room temperature, Science 286 (1999) 1227–1229.
[5] J. Hilding, E.A. Grulke, S.B. Sinnott, D. Qian, R. Andreews, M. Jagtoyen, Sorption of butane on carbon multiwall nanotubes at room temperature, Langmuir 17 (2001) 7540–7544.
[6] L. Schlapbach, A. Züttel, Hydrogen-storage materials for mobile applications, Nature (Lond.) 414 (2001) 353–358.
[7] H.M. Cheng, Q.H. Yang, C. Liu, Hydrogen storage in carbon nanotubes, Carbon 39 (2001) 1447–1454.
[8] R.Q. Long, R.T. Yang, Carbon nanotubes as superior sorbent for dioxin removal, J. Am. Chem. Soc. 123 (2001) 2058–2059.
[9] Z.W. Liu, Y. Gao, Y. Bando, Hydrogen storage in single-walled carbon nanotubes at room temperature, Science 286 (1999) 1227–1229.
[10] K. Yang, L. Zhou, B. Xing, Adsorption of polycylic aromatic hydrocarbons by carbon nanomaterial, Environ. Sci. Technol. 40 (2006) 1855–1861.
[11] H. Yan, A. Gong, H. He, J. Zhou, Y. Wei, L. Lv, Adsorption of microcystins by carbon nanotubes, Chemosphere 62 (2006) 142–148.
[12] Y. Li, S. Wang, J. Wei, X. Zhang, C. Xu, Z. Luan, D. Wu, B. Wei, Lead adsorption on carbon nanotubes, Chem. Phys. Lett. 357 (2002) 263–266.
[13] Y. Li, S. Wang, Z. Luan, J. Ding, C. Xu, D. Wu, Adsorption of cadmium(II) from aqueous solution by surface oxidized carbon nanotubes, Carbon 41 (2003) 1057–1062.
[14] Y. Li, Z. Luan, X. Xiao, X. Zhou, C. Xu, D. Wu, B. Wei, Removal Cu^{2+} ions from aqueous solutions by carbon nanotubes, Adsorp. Sci. Technol. 21 (2003) 475–485.
[15] Y. Li, J. Ding, Z. Lun, Z. Di, Y. Zhu, C. Xu, D. Wu, B. Wei, Competitive adsorption of Pb^{2+}, Cu^{2+} and Cd^{2+} ions from aqueous solutions by multiwalled carbon naotubes, Carbon 41 (2003) 2787–2792.
[16] Y. Li, Z. Di, J. Ding, D. Wu, Z. Luan, Y. Zhu, Adsorption thermodynamic, kinetic and desorption studies of Pb^{2+} on carbon nanotubes, Water Res. 39 (2005) 605–609.
[17] X.K. Wang, C.L. Chen, W.P. Hu, A.P. Ding, D. Xu, X. Zhou, Sorption of ^{243}Am(III) to multiwall carbon nanotubes, Environ. Sci. Technol. 39 (2005) 2856–2860.
[18] C.L. Chen, X.K. Wang, Adsorption of Ni(II) from aqueous solution using oxidized multiwall carbon nanotubes, Ind. Eng. Chem. Res. 45 (2006) 9144–9149.

[19] C. Lu, H. Chiu, Adsorption of zinc(II) from water with purified carbon nanotubes, Chem. Eng. Sci. 61 (2006) 1138–1145.
[20] C. Lu, H. Chiu, C. Liu, Removal of Zinc(II) from aqueous solution by purified carbon nanotubes: kinetics and equilibrium studies, Ind. Eng. Chem. Res. 45 (2006) 2850–2855.
[21] Y. Li, S. Wang, A. Cao, D. Zhao, X. Zhang, C. Xu, Z. Luan, D. Ruan, J. Liang, D. Wu, B. Wei, Adsorption of fluoride from water by amorphous alumina supported on carbon nanotubes, Chem. Phys. Lett. 350 (2001) 412–416.
[22] X. Peng, Z. Luan, Z. Di, Z. Zhang, C. Zhu, Carbon nanotubes–iron oxides magnetic composites as adsorbent for removal of Pb(II) and Cu(II) from water, Carbon 43 (2005) 880–883.
[23] W. Wang, P. Serp, P. Kalck, J.L. Faria, Photocatalytic degradation of phenol on MWNT and titania composite catalysts prepared by a modified sol–gel method, Appl. Catal. B 56 (2005) 305–312.
[24] X. Xia, Z. Jia, Y. Yu, Y. Liang, Z. Wang, L. Ma, Preparation of multi-walled carbon nanotube supported TiO_2 and its photocatalytic activity in the reduction of CO_2 with H_2O, Carbon 45 (2007) 717–721.
[25] Z.C. Di, J. Ding, X.J. Peng, Y.H. Li, Z.K. Luan, J. liang, Chromium adsorption by aligned carbon nanotubes supported ceria nanoparticles, Chemosphere 62 (2006) 861–865.
[26] X.L. Tan, M. Fang, X.K. Wang, Preparation of TiO_2/multiwalled carbon nanotube composites and its application in photocatalytic reduction of Cr(VI) study, J. Nanosci. Nanotechnol. 8 (2008) 1–8.
[27] N.A. Booker, D. Keir, A. Priestley, C.D. Rithchie, Sewage clarification with magnetite particles, Water Sci. Technol. 23 (1991) 1703–1712.
[28] K.S. Sing, Technology profile, Ground Water Monit. (1994) 60–76.
[29] I. Safarik, M. Safarikova, V. Buricova, Sorption of water soluble organic dyes on magnetic poly(oxy-2,6-dimethyl-1,4-phenylene), Collect. Czech. Chem. Commun. 60 (1995) 1448–1456.
[30] J.D. Orbell, L. Godhino, S.W. Bigger, T.M. Nguyen, N. Lawrence, Oil spill remediation using magnetic particles, J. Chem. Educ. 74 (1997) 1446–1450.
[31] L.C.A. Oliveira, R.V.R.A. Rios, J.D. Fabris, V.K. Garg, K. Sapag, R.M. Lago, Activated carbon/oxide magnetic composites for the adsorption of contaminants in water, Carbon 40 (2002) 2177–2183.
[32] T. Cole, G. Bidoglio, M. Soupioni, M. O'Gorman, N. Gibson, Diffusion mechanisms of multiple strontium species in clay, Geochim. Cosmochim. Acta 64 (2000) 385–396.
[33] M.A. Montes-Morán, J.A. Menéndez, E. Fuente, D. Suárez, Contribution of the basal planes to carbon basicity: an ab initio study of the H_3O^+–π interaction in cluster models, J. Phys. Chem. B 102 (1998) 595–5601.
[34] J. Rivera-Utrilla, M. Sáncher-Polo, Adsorption of Cr (III) on ozonised activated carbon. Importance of Cπ–cation interactions, Water Res. 37 (2003) 3325–3340.
[35] Z. Reddad, C. Gerente, Y. Andres, L.P. Cloirec, Adsorption of several metal ions onto a low-cost biosorbent: kinetic and equilibrium studies, Environ. Sci. Technol. 36 (2002) 2067–2073.